Progress of Theoretical Physics, Vol. 128, No. 3, September 2012

Charge-Exchange Excitations with Skyrme Interactions in a Separable Approximation

Alexey P. Severyukhin,[1] Victor V. Voronov[1] and Nguyen Van Giai[2]

[1]*Bogoliubov Laboratory of Theoretical Physics, Joint Institute for Nuclear Research, 141980 Dubna, Moscow Region, Russia*
[2]*Institut de Physique Nucléaire, CNRS-IN2P3 and Univ. Paris-Sud, 91405 Orsay, France*

(Received May 3, 2012; Revised July 11, 2012)

Starting from a Skyrme interaction we propose an extension of the finite rank separable approximation for the case of charge-exchange nuclear modes. This approximation enables one to reduce considerably the dimensions of the matrices that must be diagonalized to perform QRPA calculations in very large configuration spaces. First, we check that the approximation reproduces reasonably well the full charge-exchange RPA results of the spin-dipole resonances in the nuclei ^{90}Zr and ^{132}Sn. The approach is then applied to the study of the Gamow-Teller and the spin-dipole resonances in the neutron-rich Cd isotopes, within the quasiparticle random phase approximation.

Subject Index: 210, 213

§1. Introduction

The study of spin-isospin excitations in neutron-rich nuclei is presently an important problem not only from the nuclear structure point of view but also because of the special role they play in many astrophysical processes. Many fundamental issues depend on our quantitative understanding of phenomena like beta decays of nuclei, nuclear electron capture or the r-process in nucleosynthesis. It is desirable to have theoretical models which can describe the data wherever they can be measured and which can predict the properties related to spin-isospin excitations in systems too short-lived to allow for experimental studies.

Recent progress in measurements of charge-exchange modes have stimulated developments of the nuclear models. For example, the neutron skin thickness of nuclei could be in principle obtained from data on properties of spin-dipole (SD) excitations.[1)–3)] If such neutron skin measurements could be done on ^{208}Pb one would have an independent and accurate check of the expected results from the ambitious PREX project at CEBAF[4),5)] and thus, a reliable determination of the density dependence of the nuclear symmetry energy.

At the same time, the experimental studies using the multipole decomposition analysis (MDA) of the (n,p) and (p,n) reactions[2),3),6)] have clarified the longstanding problem of the missing experimental Gamow-Teller (G-T) strength in nuclei,[7),8)] hence resolving the discrepancy between the random phase approximation (RPA) predictions and G-T measurements. Thus, the field of charge-exchange nuclear excitations is a cornerstone in the study of atomic nuclei, and it is our purpose here

to propose a method which can simplify the microscopic calculations of such excited states.

The quasiparticle random phase approximation (QRPA) with the Skyrme interaction is a standard microscopic approach in nuclear structure theory.[9),10)] Many charge-exchange versions of it were developed during the last decade.[7),8),11)–16)] Their common feature is that they allow to relate the properties of the ground states and excited states through the same energy density functional. On the other hand, it would be desirable to extend the description beyond the QRPA scheme in order to include damping effects observed experimentally. There have been such attempts in the past[17),18)] which allow one to understand the damping of charge-exchange resonances and their particle decay. Recently, the damping of the G-T mode was investigated using Skyrme RPA plus particle-vibration coupling.[19)] However, the size of the configuration space increases very rapidly and one has to study only a limited number of typical cases. It would be helpful to have an approach where the size of the calculations does not depend directly on the size of the configuration space. At the RPA and QRPA levels such approaches were introduced many years ago by Brown and Bolsterli[20)] and by Soloviev et al.[21)–23)] using a separable form for the residual particle-hole (p-h) interaction.

More recently, several attempts have been made to reduce the numerical effort when performing RPA and QRPA calculations with Skyrme-type interactions. One type of simplification is to replace the full p-h Skyrme interaction by a finite sum of products of one-body operators appropriately chosen.[24)–26)] Another type which is well suited for spherically symmetric systems is the so-called finite rank separable approximation (FRSA) for the Skyrme p-h residual interaction.[27),28)] The FRSA has been used to study the electric low-lying states and giant resonances within the QRPA and beyond.[29),30)] Alternative schemes to factorize the p-h interaction have also been applied to the study of the deformation effects on the β-decay properties.[31),32)]

In this paper we introduce the FRSA to the QRPA description of charge-exchange excitation modes, and especially of spin-isospin excitations, in spherical nuclei. The aim of this work is first to present the method and to assess its accuracy by comparing its results to calculations done with the complete p-h Skyrme interaction. Then, we apply the FRSA to calculate G-T and SD strength distributions in the T_+ and T_- channels, in some neutron-rich Cd isotopes.

This paper is organized as follows: in §2 we sketch our method and we show how to use the FRSA in charge-exchange QRPA. The explicit solution of the corresponding QRPA equations is given. In §3 the FRSA is checked on the properties of the GTR and the SDR in some spherical nuclei. Results of QRPA calculations for the GTR and SDR in $^{126-130}$Cd are discussed in §4. Conclusions are drawn in §5.

§2. Finite rank approximation for charge-exchange modes

The RPA and QRPA methods within the FRSA have been introduced in Refs. 27) and 29). In this section we present their extension to the case of charge-exchange excitations.[33),34)] The quasiparticle states are labelled by $\boldsymbol{a}, \boldsymbol{b}, \ldots$ ($\boldsymbol{\alpha}, \boldsymbol{\beta}, \ldots$) for neu-

tron (proton) states. Assuming spherical symmetry for the nuclei considered here, each state $\boldsymbol{a} = (a, m_a)$ is defined by the quantum numbers $a = \{E_a, l_a, j_a\}$ and the angular momentum projection m_a. Here, $E_a = (\epsilon_a^2 + \Delta_a^2)^{1/2}$ is the corresponding quasiparticle energy expressed in terms of the Hartree-Fock (HF) single-particle energy ϵ_a and pairing energy Δ_a. The starting point of the method is the HF-BCS description[35] of the parent ground state. The method could be extended to the Hartree-Fock-Bogoliubov (HFB) framework and the corresponding QRPA equations would have the same structure if one expresses them in the canonical quasiparticle basis. Denoting by $c_{\boldsymbol{a}}^+, c_{\boldsymbol{a}}$ (resp. $c_{\boldsymbol{\alpha}}^+, c_{\boldsymbol{\alpha}}$) the creation and annihilation operators of a neutron (resp. proton) in a single-particle state, the creation and annihilation operators of neutron quasiparticles – $d_{\boldsymbol{a}}^+, d_{\boldsymbol{a}}$ – are obtained by the canonical Bogoliubov transformation:

$$c_{\boldsymbol{a}}^+ = u_a d_{\boldsymbol{a}}^+ + (-1)^{j_a - m_a} v_a d_{\boldsymbol{a}'} \ , \tag{2·1}$$

where $\boldsymbol{a}' \equiv (a, -m_a)$, and u_a, v_a are the BCS amplitudes. Similar relations apply for the proton states.

To each quasiparticle state $\boldsymbol{a}$ corresponds a HF wave function:

$$\varphi_{\boldsymbol{a}}(r, \boldsymbol{\sigma}) = \frac{f_a(r)}{r} \mathcal{Y}_{\boldsymbol{a}}(\hat{r}, \sigma) \ . \tag{2·2}$$

In practice, the HF mean field is calculated with a Skyrme-type interaction whereas the BCS equations are solved self-consistently with a density-dependent, zero-range pairing force of the type:[36]

$$V_{pair}(\boldsymbol{r}_1, \boldsymbol{r}_2) = V_0 \left(1 - \eta \left(\frac{\rho\,(r_1)}{\rho_0}\right)^{\alpha}\right) \delta\,(\boldsymbol{r}_1 - \boldsymbol{r}_2) \ , \tag{2·3}$$

where V_0, η, α are adjusted parameters, $\rho(r)$ is the HF-BCS ground state density, ρ_0 being the nuclear matter saturation density. The parameters are determined by adjusting the empirical odd-even mass differences of the nuclei in the region under study. One thus obtains the sets of proton and neutron quasiparticle states, $\boldsymbol{\alpha}$ and $\boldsymbol{a}$, with the corresponding wave functions ($\varphi_{\boldsymbol{\alpha}}$ and $\varphi_{\boldsymbol{a}}$), quasiparticle energies (E_α and E_a) and BCS amplitudes (u_α, v_α and u_a, v_a). The continuum part of the quasiparticle spectrum is generally discretized by various methods like harmonic oscillator expansion or box boundary conditions.

To build the QRPA equations on the basis of quasiparticle states as defined above and using consistently the residual interactions (derived from the Skyrme force in the particle-hole channel and from the zero-range pairing force in the particle-particle channel) is a standard procedure.[9] This leads to the familiar QRPA equations in configuration space:

$$\begin{pmatrix} \mathcal{A} & \mathcal{B} \\ -\mathcal{B} & -\mathcal{A} \end{pmatrix} \begin{pmatrix} X \\ Y \end{pmatrix} = \omega \begin{pmatrix} X \\ Y \end{pmatrix} \ , \tag{2·4}$$

where the dimensions of the matrices $\mathcal{A}$ and $\mathcal{B}$ grow very rapidly with the size of the nuclear system unless severe and damaging cutoffs are made to the 2-quasiparticle configuration space. It is well known that, if the matrix elements of the $\mathcal{A}$ and $\mathcal{B}$

matrices take a separable form the eigenvalues of Eq. (2·4) can be obtained as the roots of a relatively simple secular equation.[20),23)] In the case of the Skyrme interaction this feature has been exploited by different authors.[24),25),27)] In particular, a method has been proposed in Refs. 27) and 29) to calculate non charge-exchange excitations, and we extend here this method to the case of non closed-shell nuclei and charge-exchange excitations. The main step is to replace the Skyrme particle-hole interaction by its Landau-Migdal approximation and to keep only the $l = 0$ terms. We recall that the central terms of the Skyrme force do not act in states with relative momentum $l \geq 2$. It has been shown[14)] that the effect of the two-body spin-orbit residual interaction on the G-T excitations is small, and furthermore, we do not consider here versions of the force having a two-body tensor component. Thus, keeping only $l = 0$ might not be that bad, and this will be discussed in the next section.

We write the p-h interaction in the spin-isospin channel in the following form:

$$V_{res}(\boldsymbol{r}_1, \boldsymbol{r}_2) = N_0^{-1}[F_0^{'}(r_1) + G_0^{'}(r_1)\boldsymbol{\sigma}^{(1)} \cdot \boldsymbol{\sigma}^{(2)}]\boldsymbol{\tau}^{(1)} \cdot \boldsymbol{\tau}^{(2)}\delta(\boldsymbol{r}_1 - \boldsymbol{r}_2) \ , \qquad (2\cdot5)$$

where $\boldsymbol{\sigma}^{(i)}$ and $\boldsymbol{\tau}^{(i)}$ are the spin and isospin operators, and $N_0 = 2k_F m^*/\pi^2\hbar^2$ with k_F and m^* standing for the Fermi momentum and nucleon effective mass in nuclear matter. $F_0^{'}, G_0^{'}$ are functions of the position $\boldsymbol{r}$ through their density dependence, and their expressions in terms of the Skyrme force parameters can be found in Ref. 37).

When calculating particle-hole matrix elements of the interaction (2·5) one obtains a sum of products of angular momentum coefficients times one-dimensional radial integrals. These integrals are numerically calculated by choosing a large enough cutoff radius R and using an N-point integration Gauss formula with abscissas r_k and weights w_k.[27)] Thus, one is led to deal with a problem where the $V_{ph,p'h'}$ matrix elements are sums of products, $\Sigma_n V_{ph}(n)V_{p'h'}(n)$, and the number $\tilde{N}$ of terms in the sums depends only on N ($\tilde{N} = 4N$ for the cases studied here). One can call it a separable approximation of finite rank $\tilde{N}$ since finding the roots of the secular equation amounts to find the zeros of a $\tilde{N} \times \tilde{N}$ determinant, and the dimensions of the determinant are independent of the size of the configuration space, i.e., of the nucleus considered.

Let us briefly explain the main steps leading to the FRSA solutions of the QRPA equations. Our goal is to express the matrix elements of the angular momentum coupled matrices $\mathcal{A}_{a\alpha,b\beta}$ and $\mathcal{B}_{a\alpha,b\beta}$ appearing in the QRPA equations (2·4) as sums of products of terms depending on (a, α) or (b, β). We separate in the calculations the cases of natural parity states ($L = J$) and unnatural parity states ($L = J \pm 1$), where L and J are the orbital and total angular momenta of the excitations considered. First, we introduce the interaction strengths $\kappa_F^{(k)}, \kappa_G^{(k)}$ at points r_k by the following definitions:

$$\begin{pmatrix} \kappa_F^{(k)} \\ \kappa_G^{(k)} \end{pmatrix} = -N_0^{-1}\frac{Rw_k}{2r_k^2}\begin{pmatrix} F_0^{'}(r_k) \\ G_0^{'}(r_k) \end{pmatrix}, \qquad (2\cdot6)$$

where all quantities are defined in the preceding paragraph. Next, we introduce the quantities $h_{a\alpha}^{J,k}$ and $g_{a\alpha}^{LJ,k}$ which are related to reduced matrix elements of the operators Y_J and $T_{LJ} = (Y_L \otimes \boldsymbol{\sigma})_J$, respectively:

$$h_{a\alpha}^{(J,k)} = f_a(r_k)f_\alpha(r_k)\langle a||i^J Y_J||\alpha\rangle,$$

Table I. The coefficients $\kappa^{(n)}$ (resp. $d^{(n)}_{a\alpha}$) appearing in Eq. (2·8) expressed in terms of the quantities defined in Eq. (2·6) (resp. Eq. (2·7)). The index k runs from 1 to the number of Gauss points N.

	$L = J \pm 1$		$L = J$	
n	$\kappa^{(n)}$	$d^{(n)}_{a\alpha}$	$\kappa^{(n)}$	$d^{(n)}_{a\alpha}$
k	$\kappa^{(k)}_G$	$g^{(J-1,J,k)}_{a\alpha}$	$\kappa^{(k)}_G$	$g^{(J,J,k)}_{a\alpha}$
$k+N$	$\kappa^{(k)}_G$	$g^{(J+1,J,k)}_{a\alpha}$	$\kappa^{(k)}_F$	$h^{(J,k)}_{a\alpha}$

$$g^{(L,J,k)}_{a\alpha} = f_a(r_k) f_\alpha(r_k) \langle a||i^L T_{LJ}||\alpha\rangle \ . \tag{2·7}$$

Now, the matrix elements of the QRPA matrices take the form:

$$\mathcal{A}_{a\alpha,b\beta} = -2\hat{J}^{-2}(u_a v_\alpha u_b v_\beta + v_a u_\alpha v_b u_\beta) \sum_{n=1}^{2N} \kappa^{(n)} d^{(n)}_{a\alpha} d^{(n)}_{b\beta} + \varepsilon_{a\alpha}\delta_{ab}\delta_{\alpha\beta} \ ,$$

$$\mathcal{B}_{a\alpha,b\beta} = -2\hat{J}^{-2}(u_a v_\alpha v_b u_\beta + v_a u_\alpha u_b v_\beta) \sum_{n=1}^{2N} \kappa^{(n)} d^{(n)}_{a\alpha} d^{(n)}_{b\beta} \ . \tag{2·8}$$

Here, $\hat{J} = \sqrt{2J+1}$ and the 2-quasiparticle energies are $\varepsilon_{a\alpha} = E_a + E_\alpha$. The $\kappa^{(n)}$ interaction strengths and $d^{(n)}_{a\alpha}$ matrix elements in Eq. (2·8) are defined in Table I.

Now, we show how to construct the secular equation in a determinantal form. In the $4N$-dimensional space we introduce a vector $\begin{pmatrix} D_+ \\ D_- \end{pmatrix}$ by its components:

$$D^{\nu n}_{\pm} = \sum_{a\alpha} d^{(n)}_{a\alpha} u^{(\pm)}_{a\alpha} \left(X^\nu_{a\alpha} \pm Y^\nu_{a\alpha}\right), \tag{2·9}$$

where $u^{(\pm)}_{a\alpha} = u_a v_\alpha \pm v_a u_\alpha$, $n = 1, 2, ...2N$, and the index ν refers to the ν-th QRPA state. The QRPA amplitudes (X, Y) can be expressed in terms of the $D_\pm$ as:

$$X^\nu_{a\alpha} = \frac{1}{\varepsilon_{a\alpha} - \omega_\nu} \sum_{n=1}^{2N} d^{(n)}_{a\alpha} \kappa^{(n)} \left(D^{\nu n}_+ u^{(+)}_{a\alpha} + D^{\nu n}_- u^{(-)}_{a\alpha} \right) \ , \tag{2·10}$$

$$Y^\nu_{a\alpha} = \frac{1}{\varepsilon_{a\alpha} + \omega_\nu} \sum_{n=1}^{2N} d^{(n)}_{a\alpha} \kappa^{(n)} \left(D^{\nu n}_+ u^{(+)}_{a\alpha} - D^{\nu n}_- u^{(-)}_{a\alpha} \right) \ . \tag{2·11}$$

Now, the QRPA equations (2·4) become:

$$\begin{pmatrix} \mathcal{M}_1 - \frac{1}{2}I & \mathcal{M}_2 \\ \mathcal{M}_2 & \mathcal{M}_3 - \frac{1}{2}I \end{pmatrix} \begin{pmatrix} \mathcal{D}_+ \\ \mathcal{D}_- \end{pmatrix} = 0 \ , \tag{2·12}$$

where the matrix elements of the $2N \times 2N$ matrices $\mathcal{M}_k$ $(k = 1, 2, 3)$ have the following expressions:

$$\mathcal{M}^{nn'}_1 = \frac{\kappa^{(n')}}{\hat{J}^2} \sum_{a\alpha} \frac{d^{(n)}_{a\alpha} d^{(n')}_{a\alpha} \left(u^{(+)}_{a\alpha}\right)^2 \varepsilon_{a\alpha}}{\varepsilon^2_{a\alpha} - \omega^2} \ , \tag{2·13}$$

$$\mathcal{M}_2^{nn'} = \frac{\kappa^{(n')}}{\hat{J}^2} \sum_{a\alpha} \frac{d_{a\alpha}^{(n)} d_{a\alpha}^{(n')} u_{a\alpha}^{(+)} u_{a\alpha}^{(-)} \omega}{\varepsilon_{a\alpha}^2 - \omega^2} \ , \tag{2·14}$$

$$\mathcal{M}_3^{nn'} = \frac{\kappa^{(n')}}{\hat{J}^2} \sum_{a\alpha} \frac{d_{a\alpha}^{(n)} d_{a\alpha}^{(n')} \left(u_{a\alpha}^{(-)}\right)^2 \varepsilon_{a\alpha}}{\varepsilon_{a\alpha}^2 - \omega^2} \ . \tag{2·15}$$

The eigenvalues ω of Eq. (2·4) are the roots of the equation:

$$\det \begin{pmatrix} \mathcal{M}_1 - \frac{1}{2}I & \mathcal{M}_2 \\ \mathcal{M}_2 & \mathcal{M}_3 - \frac{1}{2}I \end{pmatrix} = 0. \tag{2·16}$$

Since the vector $\begin{pmatrix} D_+ \\ D_- \end{pmatrix}$ satisfies Eq. (2·12) the QRPA amplitudes $X_{a\alpha}^{\nu}, Y_{a\alpha}^{\nu}$ are obtained by Eqs. (2·10), (2·11) and the normalization condition:

$$\sum_{a\alpha} |X_{a\alpha}^{\nu}|^2 - |Y_{a\alpha}^{\nu}|^2 = 1 \ . \tag{2·17}$$

The excitation energies with respect to the parent ground state are

$$E_{\nu}^{\mp} = \omega_{\nu} \mp (\lambda_n - \lambda_p) \, , \tag{2·18}$$

where ω_{ν} denotes the QRPA energies in the $T_{\mp}$ channels, λ_n and λ_p being the neutron and the proton chemical potentials, respectively.

§3. Quantitative check of the FRSA

In this section we evaluate the accuracy of the FRSA by comparing results obtained using this separable approximation with those from a full treatment of the Skyrme-type p-h residual interaction. In the literature one can find full charge-exchange calculations of SD states built on ^{90}Zr, carried out either in RPA[7] or in RPA and TDA.[14] We select the SD transitions in the T_- and T_+ channels from the parent ground states of ^{90}Zr and ^{132}Sn as illustrative cases. For the sake of simplicity the check is done within the Tamm-Dancoff approximation (TDA) without pairing effects. The RPA results would be similar because the backward-going graphs are somewhat blocked in these charge-exchange channels, and in any case we are just interested here in assessing the validity of the FRSA.

The calculations are done with the Skyrme parameter set SGII[37] which was designed to give reasonable values for the spin-isospin Landau parameters. In Eq. (2·5) F_0' and G_0' at saturation density are equal to 0.73 and 0.50, respectively. The HF mean field is first calculated in coordinate space, then the single-particle spectra necessary for the TDA calculations (energies and wave functions) are obtained by diagonalizing the HF mean field in a 12-shells harmonic oscillator basis and keeping all states below 100 MeV. This is sufficient to exhaust the Ikeda sum rule $3(N-Z)$[38] for the G-T strength as well as the SD sum rule:[1),2)]

$$S_- - S_+ = \frac{9}{4\pi} \left(N\langle r^2 \rangle_n - Z\langle r^2 \rangle_p \right) \ , \tag{3·1}$$

Table II. SD sum rule values in ^{90}Zr and ^{132}Sn, expressed in fm^2. $S(r_n, r_p)$ stands for the r.h.s. of Eq. (3·1). The experimental data are taken from Refs. 2) and 7).

		r_n (fm)	r_p (fm)	$S(r_n, r_p)$	S_-	S_+	$S_- - S_+$
^{90}Zr	full	4.253	4.198	142.9	279.2	135.7	143.4
	FRSA	4.253	4.198	142.9	279.6	136.0	143.7
	Expt.				271±14	124±11	147±13
^{132}Sn	full	4.856	4.658	607.7	694.3	87.3	607.1
	FRSA	4.856	4.658	607.7	694.3	87.3	607.1

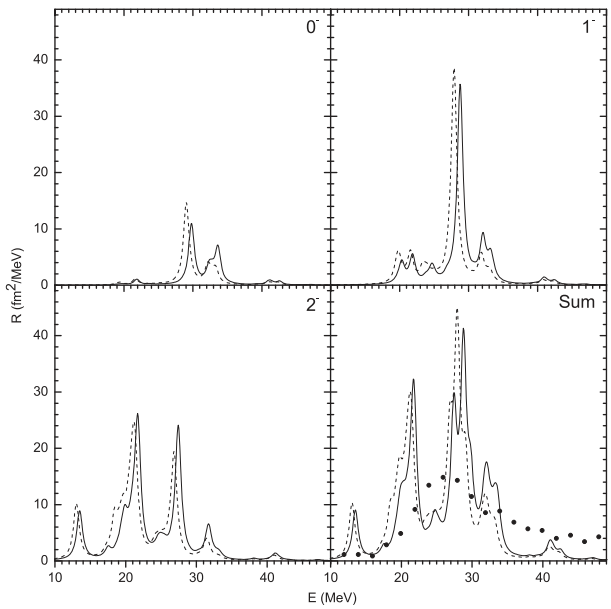

Fig. 1. Spin-dipole strength distributions in the T_- channel of the parent nucleus ^{90}Zr. The results with the FRSA for the p-h interaction (dashed lines), and with the full p-h interaction (solid lines) are shown. The experimental data shown by the black dots are taken from Refs. 2) and 7).

where

$$S_\mp = \sum_\nu |\langle N \mp 1, Z \pm 1; \nu | \hat{O}_\mp | N, Z \rangle|^2 \tag{3·2}$$

are the total SD transition strengths to the neighbouring daughter nuclei induced by the operators

$$\hat{O}_\mp = \sum_{i,m,\mu} r_i t_\mp(i) \sigma_m(i) Y_1^\mu(\hat{r}_i) \ . \tag{3·3}$$

From our previous studies of the FRSA applied to non charge-exchange excitations[28),30)] we could conclude that a value $N = 45$ for the number of Gauss points in the radial integrals is sufficient for the desired accuracy in all nuclei with $A \leq 208$.

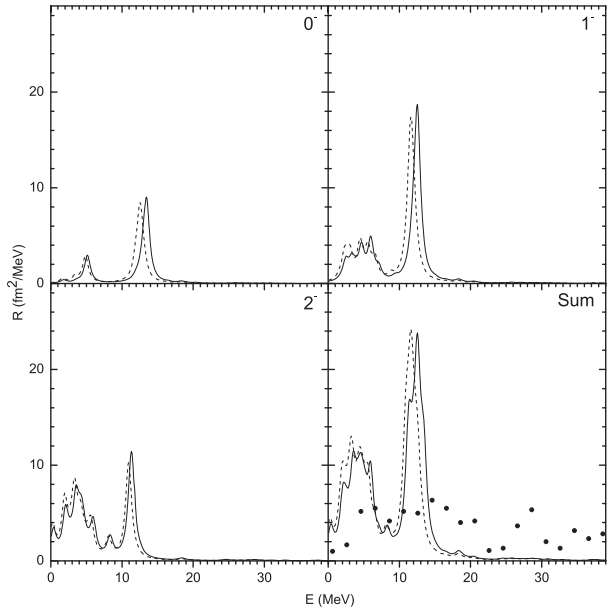

Fig. 2. Same as Fig. 1, for the T_+ channel.

For example, choosing $N = 60$ would change the calculated energies and transition probabilities by less than 1%. Thus, we adopt here the value $N = 45$. All calculations are without any quenching factor. In the figures, the calculated strength distributions are folded out with a Lorentzian distribution of 1 MeV width.

In Table II, we compare the SD sum rule (3·1) calculated in FRSA and with the full SGII force. To compare with experimental data in ^{90}Zr we choose the energy interval $E \leq 50$ MeV for the T_- channel and $E \leq 26$ MeV for the T_+ channel.[2),7)] One can see that the FRSA sum rules are quite close to those of the full calculations. The calculated values S_-, S_+ agree well with experimental data[2),7)] in ^{90}Zr. In ^{132}Sn a perfect agreement is obtained between the r.h.s. of Eq. (3·1) and the l.h.s. calculated either in FRSA or full Skyrme TDA.

The SD sum rule (3·1) is an integral characteristic and it is less sensitive to the details than the SD strength distribution. The calculated T_- and T_+ strength distributions in various J^π channels are shown in Figs. 1 and 2, for the ^{90}Zr case. The excitation energies refer to the ground state of the parent nucleus ^{90}Zr. The experimental strength distributions[2),7)] for the T_- and T_+ channels are results of the multipole decomposition analysis done for the $^{90}\mathrm{Zr}(p,n)^{90}\mathrm{Nb}$ and $^{90}\mathrm{Zr}(n,p)^{90}\mathrm{Y}$ reactions, respectively. From Figs. 1 and 2, it can be seen that the FRSA reproduces the essential features of the SD strength distributions with a downward shift about 0.9 MeV in the positions of the high energy peaks for the T_- and T_+ channels. Thus, the p-h interaction in the FRSA is slightly weaker than the original interaction. The difference between the full calculation and the FRSA is small in global

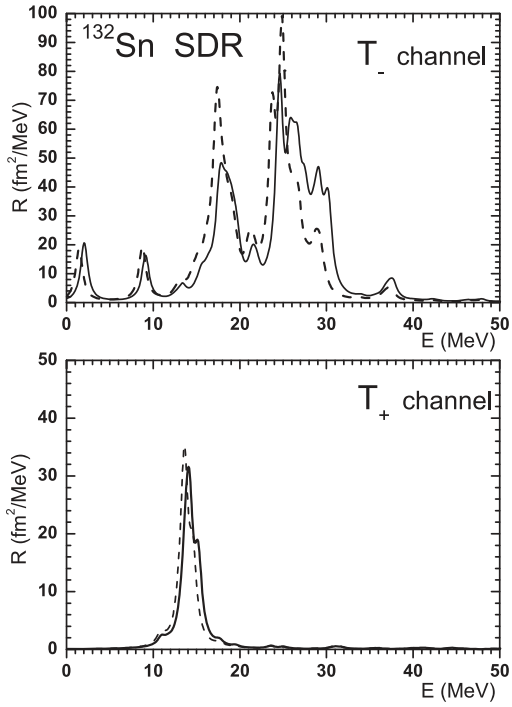

Fig. 3. The spin-dipole strength distributions summed over $J^\pi = 0^-, 1^-, 2^-$ in both $T_\mp$ channels in ^{132}Sn. Same notations as in Figs. 1 and 2.

comparison with the experimental data. There is the missing of significant part of the experimental strength distribution in the region above the main peaks. One can expect a redistribution of strength if the coupling of the 1p-1h configurations to more complex 2p-2h configurations is taken into account.[22),39),40)] The p-h interaction of the form Eq. (2·5) allows one to simplify the calculation of such couplings, and this study is now in progress. It is worth mentioning that the SD strength distributions in ^{90}Zr are rather well studied within the 1p-1h configuration space (for example, see Refs. 7), 14) and 41)). The effect of the tensor correlations on the SD strength distributions is studied in Ref. 8).

We have done a similar check of the FRSA in the case of the parent nucleus ^{132}Sn. The SD strength distributions summed over the three J^π components in both T_- and T_+ channels are shown in Fig. 3. As can be seen from Fig. 3, the FRSA treatment changes slightly the energies of the peaks in ^{132}Sb. However, we find that the general structure remains the same. The two low-lying peaks are due to the 2^- excitations. The main configuration of the peak at $E = 2.0$ MeV (1.5 MeV in the FRSA case) is $\{\pi 1g\frac{7}{2}\nu 1h\frac{11}{2}^{-1}\}$. At the same time the leading contribution of the peak at $E = 9.1$ MeV (8.8 MeV in FRSA) comes from the configuration $\{\pi 1h\frac{11}{2}\nu 1g\frac{7}{2}^{-1}\}$. The peak around $E = 17.9$ MeV is related with the collective 0^-,

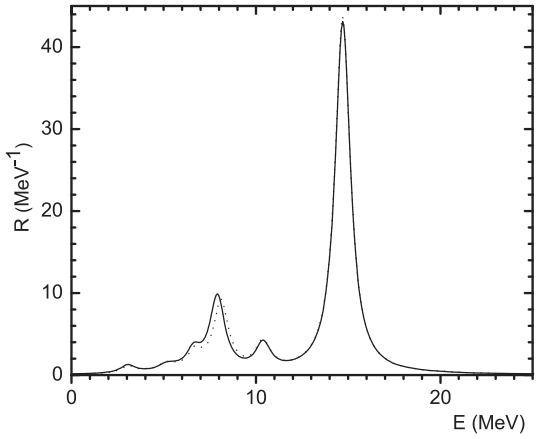

Fig. 4. Comparison of the G-T strength distribution, in ^{132}Sn, calculated with the p-h interaction (2·5) (solid line) and with the FRSA, N=15 (dotted line). See the text for the discussion.

1^-, and 2^- states. The peak energy is moved downward by about 0.5 MeV in FRSA. The main features of the high-energy broad bump are well reproduced by the FRSA. For the T_+ channel, the Pauli blocking of the neutron excess in ^{132}Sn is the reason why there is only one sharp peak in the strength distribution, and the S_+ value is much smaller than the S_- value (see Table II). The $J^\pi = 0^-$, 1^-, and 2^- states in the daughter nucleus ^{132}In are concentrated in the sharp peak at $E = 14.1$ MeV which is shifted downward by 0.5 MeV if one uses the FRSA. The 0^- and 1^- states are due to the $\{\nu 1h\frac{9}{2}\pi 1g\frac{9}{2}^{-1}\}$ configuration. The main configurations of the 2^- state are the $\{\nu 1h\frac{9}{2}\pi 1g\frac{9}{2}^{-1}\}$ and $\{\nu 2f\frac{5}{2}\pi 1g\frac{9}{2}^{-1}\}$.

One can thus conclude that the FRSA can reliably be used for the study of charge-exchange modes in the ^{90}Zr as well as ^{132}Sn regions. The computational gains brought about by the FRSA in charge-exchange modes can be illustrated by the case of ^{132}Sn where typical dimensions of RPA matrices to be diagonalized are 223, 596, 844 for 0^-, 1^-, 2^- channels whereas in FRSA the RPA eigenenergies are the roots of a determinant of dimension $4N$ where N is typically around 30-40 and independent of the spin and parity of the excitation. Another advantage is the possibility of looking only for the eigenvalues located within some energy interval. As can be seen from Fig. 4, the finite rank $N = 15$ is already large enough to reproduce the G-T strength distribution in the resonance energy interval of ^{132}Sn, for example. The solid line corresponds to the standard diagonalization procedure performed with the p-h interaction (2·5).

Table III. Ikeda sum rule values of G-T states. S_-, S_+ correspond to the T_- and T_+ channels, respectively.

		S_-	S_+	$S_- - S_+$
^{126}Cd	QRPA	90.6	0.7	89.9
	RPA	90.4	0.4	90.0
^{128}Cd	QRPA	96.6	0.6	96.0
	RPA	96.4	0.4	96.0
^{130}Cd	QRPA	102.5	0.5	102.0
	RPA	102.5	0.5	102.0

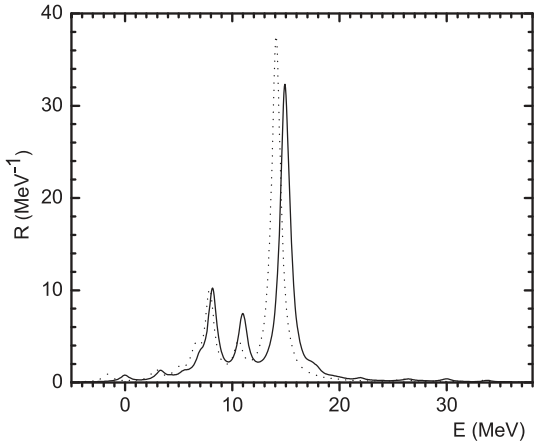

Fig. 5. Effects of pairing correlations on the G-T strength distribution in ^{126}Cd. Solid and dotted lines correspond to calculations with and without pairing correlations, respectively.

§4. Application to $^{126-130}$Cd nuclei

There is a relation between the $N = 82$ shell closure and the $A \approx 130$ peak of the solar r-process abundance distribution.[42] The $N = 82$ isotones below ^{132}Sn are important for stellar nucleosynthesis, see, e.g., Refs. 43)–46). It is interesting to study the properties of the G-T and SD states in $^{126-130}$Cd within the QRPA with Skyrme forces. In Ref. 47) the Cd isotopes were studied using the Fayans energy density functional, but the velocity-dependent parts were dropped in the Landau parameters of the spin-isospin channel. Here, we keep the contributions of the velocity-dependent terms of the p-h interaction.

First we examine the effects of the pairing correlations. We use the isospin-invariant surface-peaked pairing force (2·3), with $\eta = 1$, $\alpha = 1$ and the value $\rho_0 = 0.16$ fm^{-3} of the nuclear saturation density corresponding to the SGII force. The strength V_0 is taken equal to -870 MeV fm^3 to get a reasonable description of

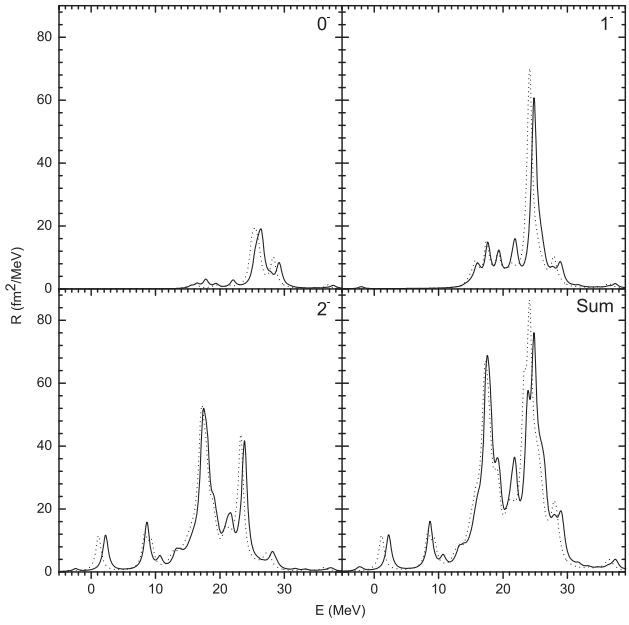

Fig. 6. Spin-dipole strength distributions in the T_- channel in ^{126}Cd, calculated in RPA and in QRPA. Same notations as in Fig. 5.

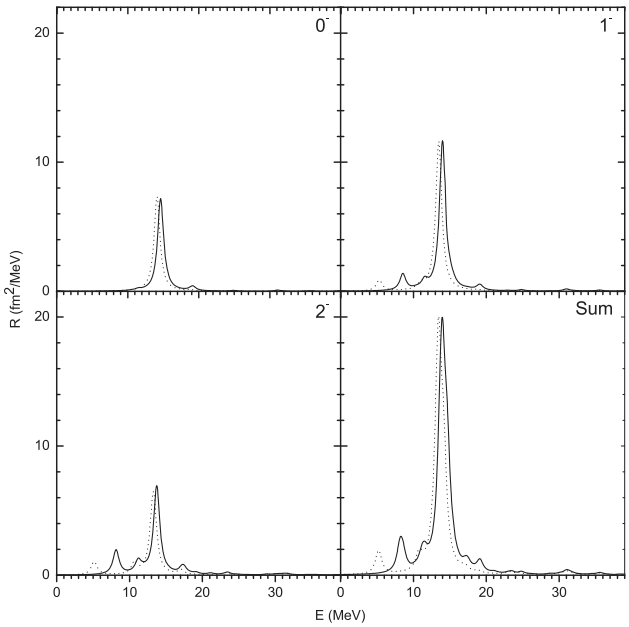

Fig. 7. Same as Fig. 6, for the T_+ channel.

Table IV. SD sum rule values in Cd isotopes, expressed in fm^2. $S(r_n, r_p)$ stands for the right-hand side of Eq. (3·1).

		r_n (fm)	r_p (fm)	$S(r_n, r_p)$	S_-	S_+	$S_- - S_+$
^{126}Cd	QRPA	4.808	4.602	563.4	621.4	56.8	564.6
	RPA	4.803	4.599	561.5	605.7	49.7	556.0
^{128}Cd	QRPA	4.831	4.614	605.4	655.8	51.5	604.3
	RPA	4.828	4.612	604.1	647.0	46.2	600.8
^{130}Cd	QRPA	4.852	4.626	647.0	688.9	46.2	642.7
	RPA	4.852	4.625	647.1	692.0	45.7	646.3

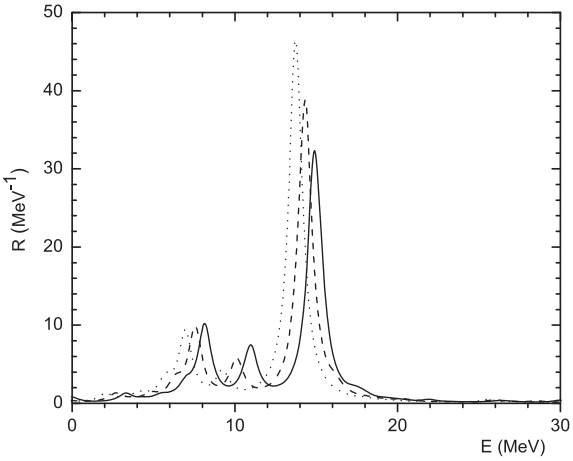

Fig. 8. The G-T strength distributions in ^{126}Cd (solid line), ^{128}Cd (dashed line), ^{130}Cd (dotted line).

the experimental pairing energies given by

$$P_N = \frac{1}{2}\left(B\left(N,Z\right) + B\left(N-2,Z\right) - 2B\left(N-1,Z\right)\right) \tag{4·1}$$

for ^{126,128}Cd. The definition of the pairing force (2·3) involves the energy cutoff of the single-particle space to restrict the active pairing space. We use the soft cutoff at 10 MeV above the Fermi energies as proposed in Refs. 29) and 48).

Results of our calculations within the RPA and QRPA for the G-T Ikeda sum rules in $^{126-130}$Cd are shown in Table III. It is worth mentioning that the RPA calculations are made by the filling approximation.[35] The pairing effects do not change the total sum rule values, but they change the contributions in separate T_- and T_+ channels. The T_+ channel is more sensitive to the changes in the pairing. As an illustration of the pairing effects on strength distributions we show in Fig. 5 the G-T strengths in ^{126}Cd calculated with and without pairing correlations. The pairing induces a 1 MeV shift of the main peak in this nucleus. Looking at the

main peak we find that the main configuration is $\{\pi 1h\frac{9}{2}\nu 1h\frac{11}{2}\}$ (65% and 61% of the QRPA and RPA wave function, respectively). The unperturbed two quasiparticle energy (resp. p-h energy) is 12.6 MeV (resp. 11.5 MeV), while the peak energy is 14.9 MeV (resp. 14.1 MeV). This seems to indicate that the difference in peak energies is due mostly to a gap effect. For ^{130}Cd, the strength distributions calculated with and without the pairing coincide. The strong difference in the neutron and proton chemical potentials plays the key role to explain this peculiarity which is rather a general feature in heavy spherical nuclei with large neutron excess.

Effects of the pairing correlations on the SD sum rules (3·1) of ^{126,128,130}Cd are shown in Table IV. Pairing effects lead to an increase of both S_+ and S_- sum rules (except for S_- in ^{130}Cd). A comparison of the calculated SD sum rule with the right-hand side of Eq. (3·1) shows that the SD sum rule is fulfilled with a good accuracy. The SD strength distributions in the T_- channel of the three J^π components in ^{126}Cd are shown in Fig. 6, while Fig. 7 shows the corresponding results for the T_+ channel. One can see that the pairing effects in ^{126}Cd lead to a slight widening of the SD resonance. On the other hand, this effect vanishes in the case of ^{130}Cd which has $N = 82$ and therefore, no neutron pairing correlations can be effective.

We turn now to the properties of G-T states in ^{126,128,130}Cd. Figure 8 shows the evolution of the G-T strength distributions in these 3 nuclei. One can see that the major part of the strength is concentrated in the peaks at $E = 14.9$, 14.3, and 13.8 MeV for ^{126}Cd, ^{128}Cd, and ^{130}Cd, respectively. The largest contribution in the peaks comes from the configuration $\{\pi 1h\frac{9}{2}\nu 1h\frac{11}{2}\}$. About 99% of the G-T strength distribution is located below 30 MeV with respect to the parent ground state. Taking into account the QRPA tensor correlations within our approach[49] can improve the results. The tensor correlations can shift up about 10% of the G-T strength to the higher energy region in the case of ^{90}Zr and ^{208}Pb.[15),16),49]

The evolution of the SD strength is shown in Figs. 9 and 10. Table IV shows the slight increase in the S_- value and the noticeable decrease in the S_+ value when the mass number grows. It is worth mentioning that the ratio 5 : 3 : 1 of the three J^π components of the $S_- - S_+$ value is fulfilled in our calculations. As can be seen from Fig. 9, for the T_- channel the fragmentation of the SD strength distributions increases with the value of J. The distributions are shifted to lower energies as one goes from ^{126}Cd to ^{130}Cd. In particular, the peak energy of the $J^\pi = 0^-$ mode of the SDR is 26.4, 25.7, and 25.0 MeV in ^{126}Cd, ^{128}Cd, and ^{130}Cd, respectively, and many configurations contribute to these structures. For the 1^- excitations, the shift of the main sharp peak is about 1 MeV. At the same time the contribution of the leading configuration $\{\pi 2i\frac{11}{2}\nu 1h\frac{11}{2}\}$ is decreasing from 54% for ^{126}Cd to 45% for ^{130}Cd. The spectrum of the 2^- states is fragmented in a wide energy range. There are two peaks in the strength distribution at lower energies. These low-energy excitations are of noncollective nature. In all three nuclei, the lowest peak is mainly due to the configuration $\{\pi 1g\frac{7}{2}\nu 1h\frac{11}{2}\}$, while the dominant configuration of the second one is $\{\pi 1h\frac{11}{2}\nu 1g\frac{7}{2}\}$. It is worth pointing out that these configurations induce the low-energy peaks obtained in ^{132}Sn, as is discussed above. Most of the 2^- strength is concentrated in the two peaks around 17.5(16.4) and 23.8(22.6) MeV in ^{126}Cd(^{130}Cd). Thus, the three J^π modes of the SDR in ^{126,128,130}Cd keep to the

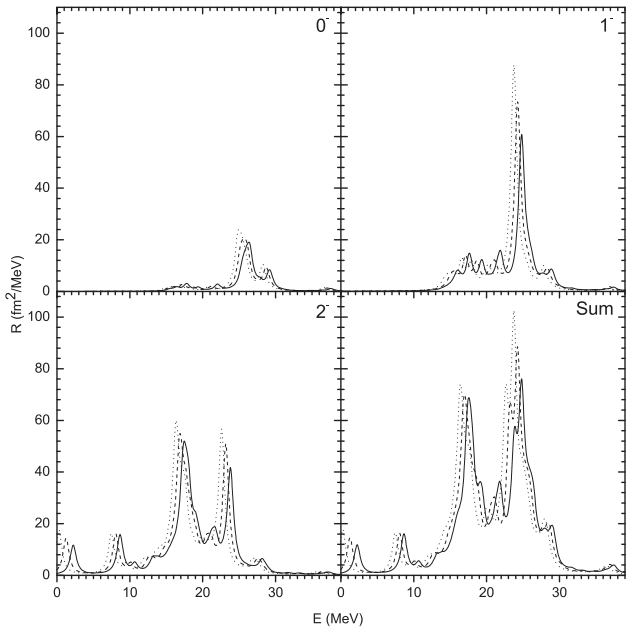

Fig. 9. Spin-dipole strength distributions of the T_- channel in ^{126}Cd (solid line), ^{128}Cd (dashed line), ^{130}Cd (dotted line).

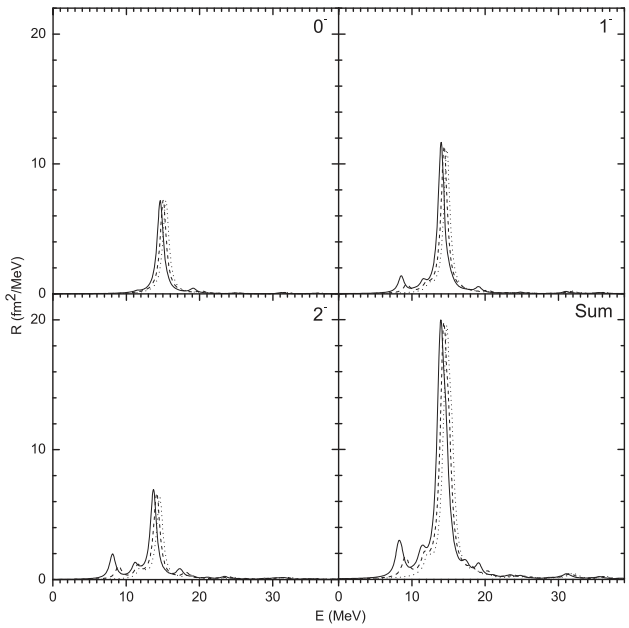

Fig. 10. Same as Fig. 9, for the T_+ channel.

energy hierarchy $E(2^-) < E(1^-) < E(0^-)$ as already found in ^{90}Zr.[7),14),41)]

The general behavior of the sharp peaks in the T_+ strength distribution is displayed in Fig. 10. With increasing mass number, the peak energy is moved upward from 14.0 MeV in ^{126}Cd to 14.8 MeV in ^{130}Cd. As expected, the Pauli blocking effect leads to a small contribution to the SD sum rule (3·1). The peaks in the 0^- and 1^- distributions have a noncollective structure with a dominant configuration $\{\nu 1h\frac{9}{2}\pi 1g\frac{9}{2}\}$. In the case of the 2^- states, the leading configurations are $\{\nu 2f\frac{5}{2}\pi 1g\frac{9}{2}\}$ and $\{\nu 1h\frac{9}{2}\pi 1g\frac{9}{2}\}$. The situation is similar to the ^{132}Sn case. The structure peculiarities of the SD strength distributions are related with the shell structure in this region of nuclei.

§5. Summary and perspectives

We have extended the finite rank separable approximation of Skyrme-type forces to the case of charge-exchange excitations, and more specifically to the spin-isospin channels. We have shown that the determination of the QRPA eigenenergies requires to calculate the zeros of a determinant whose dimensions do not depend on the size of the 2-quasiparticle configuration space. The method is validated in the case of the nuclei ^{90}Zr and ^{132}Sn by using the FRSA to calculate in TDA the Gamow-Teller and spin-dipole strength distributions in the T_+ and T_- channels, and comparing them with HF-TDA results obtained without the separable approximation.

As an application of the method we have studied the G-T and spin-dipole strength distributions of the parent nuclei ^{126,128,130}Cd in the T_+ and T_- channels by performing QRPA calculations with the FRSA and the Skyrme parametrization SGII. The effects of pairing on the spin-isospin modes are important in these nuclei, and a QRPA approach is thus appropriate. Similarly to the case of ^{90}Zr we find that the peak energies of the spin-dipole distributions in these Cd isotopes obey the energy hierarchy $E(2^-) < E(1^-) < E(0^-)$.

As an extension of the present version of the FRSA for spin-isospin modes, one should now develop a finite rank form of a tensor p-h interaction derived from a Skyrme-type tensor force,[8)] because this component of the interaction is important for these modes. One could also envisage to use the separable form of the p-h interaction to simplify the evaluation of the coupling of QRPA phonons to more complex configurations and to calculate thus the fragmentation and damping of the QRPA excitations.

Acknowledgements

We are grateful to H. Sagawa for valuable discussions. A.P.S. and V.V.V. thank for the hospitality of IPN-Orsay where a part of this work was done. This work is partly supported by the IN2P3-RFBR agreement No. 110291054.

References

1) A. Krasznahorkay et al., Phys. Rev. Lett. **82** (1999), 3216.
2) K. Yako, H. Sagawa and H. Sakai, Phys. Rev. C **74** (2006), 051303(R).

3) T. Wakasa et al., arXiv:1004.5220.
4) C. J. Horowitz, S. J. Pollock, P. A. Souder and R. Michaels, Phys. Rev. C **63** (2001), 025501.
5) K. Kumar, P. Souder, R. Michaels, K. Paschke and G. M. Urciuoli, `http://hallaweb.jlab.org/parity/prex`
6) T. Wakasa et al., Phys. Rev. C **55** (1997), 2909.
7) H. Sagawa, S. Yoshida, X.-R. Zhou, K. Yako and H. Sakai, Phys. Rev. C **76** (2007), 024301.
8) C. L. Bai, H. Q. Zhang, H. Sagawa, X. Z. Zhang, G. Colò and F. R. Xu, Phys. Rev. C **83** (2011), 054316.
9) J. Terasaki, J. Engel, M. Bender, J. Dobaczewski, W. Nazarewicz and M. Stoitsov, Phys. Rev. C **71** (2005), 034310.
10) N. Paar, D. Vretenar, E. Khan and G. Colò, Rep. Prog. Phys. **70** (2007), 691.
11) J. Engel, M. Bender, J. Dobaczewski, W. Nazarewicz and R. Surman, Phys. Rev. C **60** (1999), 014302.
12) M. Bender, J. Dobaczewski, J. Engel and W. Nazarewicz, Phys. Rev. C **65** (2002), 054322.
13) S. Fracasso and G. Colò, Phys. Rev. C **72** (2005), 064310.
14) S. Fracasso and G. Colò, Phys. Rev. C **76** (2007), 044307.
15) C. L. Bai, H. Sagawa, H. Q. Zhang, X. Z. Zhang, G. Colò and F. R. Xu, Phys. Lett. B **675** (2009), 28.
16) C. L. Bai, H. Q. Zhang, X. Z. Zhang, F. R. Xu, H. Sagawa and G. Colò, Phys. Rev. C **79** (2009), 041301(R).
17) G. Colò, Nguyen Van Giai, P. F. Bortignon and R. A. Broglia, Phys. Rev. C **50** (1994), 1496.
18) G. Colò, H. Sagawa, Nguyen Van Giai, P. F. Bortignon and T. Suzuki, Phys. Rev. C **57** (1998), 3049.
19) Y. F. Niu, G. Colò, M. Brenna, P. F. Bortignon and J. Meng, Phys. Rev. C **85** (2012), 034314.
20) G. E. Brown and M. Bolsterli, Phys. Rev. Lett. **3** (1959), 472.
21) V. A. Kuzmin and V. G. Soloviev, J. of Phys. G **10** (1984), 1507.
22) V. A. Kuzmin and V. G. Soloviev, J. of Phys. G **11** (1985), 603.
23) V. G. Soloviev, *Theory of Atomic Nuclei: Quasiparticles and Phonons* (Institute of Physics, Bristol and Philadelphia, 1992).
24) V. O. Nesterenko, J. Kvasil and P.-G. Reinhard, Phys. Rev. C **66** (2002), 044307.
25) V. O. Nesterenko, W. Kleinig, J. Kvasil, P. Vesely, P.-G. Reinhard and D. S. Dolci, Phys. Rev. C **74** (2006), 064306.
26) P. Vesely, J. Kvasil, V. O. Nesterenko, W. Kleinig, P.-G. Reinhard and V. Yu. Ponomarev, Phys. Rev. C **80** (2009), 031302.
27) Nguyen Van Giai, Ch. Stoyanov and V. V. Voronov, Phys. Rev. C **57** (1998), 1204.
28) A. P. Severyukhin, Ch. Stoyanov, V. V. Voronov and Nguyen Van Giai, Phys. Rev. C **66** (2002), 034304.
29) A. P. Severyukhin, V. V. Voronov and Nguyen Van Giai, Phys. Rev. C **77** (2008), 024322.
30) A. P. Severyukhin, V. V. Voronov and Nguyen Van Giai, Eur. Phys. J. A **22** (2004), 397.
31) P. Sarriguren, E. Moya de Guerra and A. Escuderos, Nucl. Phys. A **691** (2001), 631.
32) P. Sarriguren, E. Moya de Guerra and A. Escuderos, Phys. Rev. C **64** (2001), 064306.
33) A. P. Severyukhin, N. N. Arsenyev, V. V. Voronov and Nguyen Van Giai, Phys. At. Nuclei **72** (2009), 1149.
34) A. P. Severyukhin, V. V. Voronov and Nguyen Van Giai, J. Phys. Conf. Ser. **267** (2011), 012025.
35) P. Ring and P. Schuck, *The Nuclear Many Body Problem* (Springer, Berlin, 1980).
36) J. Dobaczewski, H. Flocard and J. Treiner, Nucl. Phys. A **422** (1984), 103.
37) Nguyen Van Giai and H. Sagawa, Phys. Lett. B **106** (1981), 379.
38) K. Ikeda, S. Fujii and J. I. Fujita, Phys. Lett. **3** (1963), 271.
39) G. F. Bertsch and I. Hamamoto, Phys. Rev. C **26** (1982), 1323.
40) S. Drözdz, F. Osterfeld, J. Speth and J. Wambach, Phys. Lett. B **189** (1987), 271.
41) Haozhao Liang, Nguyen Van Giai and Jie Meng, Phys. Rev. Lett. **101** (2008), 122502.
42) E. M. Burbidge, G. R. Burbidge, W. A. Fowler and F. Hoyle, Rev. Mod. Phys. **29** (1957), 547.
43) G. Martínez-Pinedo and K. Langanke, Phys. Rev. Lett. **83** (1999), 4502.

44) I. Dillmann et al., Phys. Rev. Lett. **91** (2003), 162503.
45) A. Jungclaus et al., Phys. Rev. Lett. **99** (2007), 132501.
46) J. J. Cuenca-García, G. Martínez-Pinedo, K. Langanke, F. Nowacki and I. N. Borzov, Eur. Phys. J. A **34** (2007), 99.
47) I. N. Borzov, Phys. Rev. C **67** (2003), 025802.
48) S. J. Krieger, P. Bonche, H. Flocard, P. Quentin and M. S. Weiss, Nucl. Phys. A **517** (1990), 275.
49) A. P. Severyukhin and H. Sagawa, in preparation.